NATIONAL UNIVERSITY OF SCIENCE AND TECHNOLOGY POLITEHNICA BUCHAREST

FACULTY OF CHEMICAL ENGINEERING AND BIOTECHNOLOGIES

DOCTORAL SCHOOL: CHEMICAL ENGINEERING AND BIOTECHNOLOGIES

DOCTORAL THESIS

- SUMMARY -

PhD coordinator:

Prof. Dr. Ing. RADU GABRIEL-LUCIAN

PhD student:

PREDA DANIEL

BUCHAREST

2025

NATIONAL UNIVERSITY OF SCIENCE AND TECHNOLOGY POLITEHNICA BUCHAREST

FACULTY OF CHEMICAL ENGINEERING AND BIOTECHNOLOGIES

DOCTORAL SCHOOL: CHEMICAL ENGINEERING AND BIOTECHNOLOGIES

ADVANCED ANALYTICAL TECHNIQUES OF DRUG DETECTION

-REZUMAT-

PhD coordinator:

Prof. Dr. Ing. RADU GABRIEL-LUCIAN

PhD student:

PREDA DANIEL

BUCHAREST

2025

Table of content

1. INTRODUCTION 4

2. ANTIBIOTICS 4

3. ANTITHROMBOTICS 5

4. ANALYTICAL TECHNIQUES USED IN INSTRUMENTAL ANALYSIS 5

5. MOLECULAR IMPRINTED POLYMERS (MIP) 6

6. ELECTROCHEMICAL SENSORS BASED ON MIPs 7

7. ELECTROCHEMICAL DETERMINATION OF OXYTETRACYCLINE USING PENCIL GRAPHITE ELECTRODE 8

8. DETERMINATION OF DIPYRIDAMOLE USING MODIFIED PENCIL GRAPHITE ELECTRODES WITH MOLECULARLY PRINTED POLYMER FILMS 9

9. ENZYMATIC DEGRADATION OF DIPYRIDAMOLE IN THE PRESENCE OF LACASE AND USING CAFFEIC ACID AS MEDIATOR. 16

10. CONCLUSIONS AND PERSONAL CONTRIBUTIONS 18

11. LIST OF PUBLICATIONS 20

12. BIBLIOGRAPHY 21

1. INTRODUCTION

Medicines are chemicals used to prevent, treat and/or relieve a wide range of conditions, acting as painkillers (which relieve pain) [1], antihypertensives (which regulate blood pressure) [2], or antidiabetics (which control blood sugar levels) [3]. They act through various biological mechanisms, influencing metabolic pathways or interacting with specific receptors in the body, to restore the functional balance of the body. Antibiotics and antithrombotics have a major role because of their profound impact on public health. Due to the excessive and inadequate use of drugs, both in terms of effect on the human body and environmental implications, the premise is outlined for the development of new methods and analytical tools for detection, quantification, study of the various processes in which these substances are involved and methods to combat pollution generated by their uncontrolled route.

2. ANTIBIOTICS

Antibiotics have become the most common category of drugs that has revolutionized medicine in recent decades. A more complex definition of antibiotics encompasses classes of molecules such as secondary metabolites of some bacterial and fungal species [4]–[6], either semi-synthetic [7]–[9] or synthetic compounds. They are divided into 2 major categories: antibiotics with **bactericidal effect** (aminoglycosides, beta-lactams, fluoroquinolones, etc.) [10] and with **bacteriostatic effect** (tetracyclines, macrolides, sulfonamides, etc.) [11]. However, this classification is not very strict, since there are also bacteriostatic antibiotics with bactericidal activity (eg linezolid) or vice versa, where bactericidal antibiotics can act as bacteriostatic under certain conditions [12].

This class of substances has a special role due to the way in which it helps living organisms to fight various bacterial infections (gastrointestinal, urinary [13], genital tract [14], skin [15], abdominal [16], central nervous system [17], ear, throat, pneumonia, typhus, bronchitis, sinusitis [9], arthritis, mastitis [4], tuberculosis, leprosy, leprosy malaria [18], etc.), thereby contributing to improving health and reducing mortality.

Unfortunately, like many other medicines, antibiotics can cause side effects such as low cell membrane permeability, fever, myalgia, hepatotoxicity and/or nephrotoxicity, rash, tendon

rupture [19],[20], hyperactivity, inflammation at the injection site [16], yellow teeth, digestive and cardiovascular disorders [21], carcinogenicity [22], etc.

3. ANTITHROMBOTICS

Antithrombotic drugs are essential in preventing arterial thrombus formation by inhibiting platelet aggregation. In the arteries, disruption of atherosclerotic plaque triggers platelet aggregation and activation of coagulation resulting in formation of platelet-rich thrombi, which obstructs blood flow (atherothrombosis) [23]. This process is the main cause of myocardial infarct, ischemic stroke and acute ischemia of the limbs. Blood flow in the veins is slower than that in the arteries, so venous platelets contain less platelets and more fibrin than arterial platelets. Blockage in the veins leads to deep vein thrombosis and pulmonary embolism, which are known as venous thromboembolism (VTE) [24].

4. ANALYTICAL TECHNIQUES USED IN INSTRUMENTAL ANALYSIS

Of the techniques used to study the properties of substances, the handiest are those based on instrumental analysis, (electrochemical and spectrometric techniques). These techniques are based on the examination of the properties of the analytes, in order to establish or confirm their structure, to elucidate the reaction mechanisms and the equilibrium involved or to estimate certain physical parameters (dissociation constant, load transfer coefficient, rate coefficient, initial reaction rate, etc.) and their quantitative determination from complex and unique matrices [25].

In electrochemical techniques and methods, which have as a central instrument the electrochemical sensor, the transducer used is the electrode, which based on proper instrumentation and method, can bring relevant information on the mechanism, as well as the quantity in which it is found in a sample of interest. The focus was on carbon-based electrodes, starting from well-known electrodes such as the glassy carbon electrode (GCE), the screen-printed carbon electrode (SPCE), the pencil graphite electrode (PGE), etc., and commencing with materials with complex structures such as graphene, graphene oxide, carbon nanomaterials (nanoparticles, quantum dots, nanowires, etc.) to highlight the current level of understanding.

Spectrometric techniques are the most widely used analytical laboratories, techniques that focus on the absorption/emission of light to bring relevant information about the reaction mechanisms in which various substances are involved and the quantities in which they are found in samples. Molecular absorption spectrometry in the visible and ultraviolet range is used to study processes involving substances with larger molecules such as drugs. At the same time, one can study the kinetics of their degradation with a role in understanding the reaction mechanism for catalyzed/biocatalized reactions. [26].

5. MOLECULAR IMPRINTED POLYMERS (MIP)

Molecularly imprinted polymers are synthesized from a template molecule (target molecule) and a functional monomer, and depending on the polymerization method are also present in the process cross-linking agents (cross-linker), porogenic solvent and reaction initiators. Functional monomers can interact to the molecule template by non-covalent interactions (hydrogen, ionic or hydrophobic bonds) or covalent (by forming structures called pre-complexes in the premerger phase of cross-linking in the porogenic solvent [4]. The main advantage of this class of polymers is the high sensitivity, conferred by the unique interaction between the analyte and the MIP.

Molecularly imprinted polymer sensors (figure 6.1) were used in the development of various detection methods (electrochemical [27], optical [28], fluorescent [29], (electro)chemiluminescence [30], surface plasmon resonance [31], ELISA [32]).

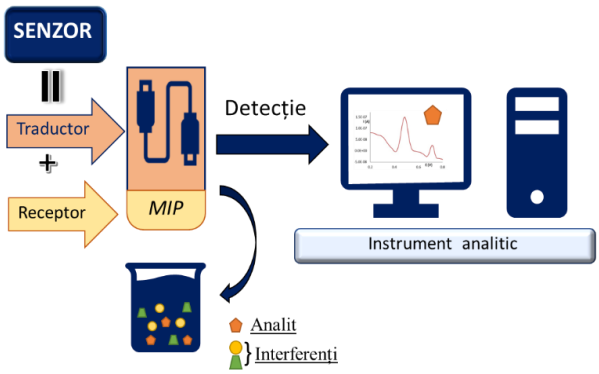

Figure 5.1. Electrochemical analysis tool and its components: receiver, transducer and analytical device.

The general procedure for the synthesis of MIPs involves 3 steps (Figure 5.2):

1) the formation of the pre-polymerization complex (pre-complex). This process is based on the combination of the template molecules with the functional monomer in the reaction solvent, with the purpose of forming covalent or non-covalent bonds;
2) initiating and propagating the polymerization process in the reaction medium, under photo/thermal conditions and in an appropriate solvent, in order to obtain a 3D polymer including target molecules.
3) removal of target molecules from the newly formed polymer, by extraction, elution or by applying an electrical potential.

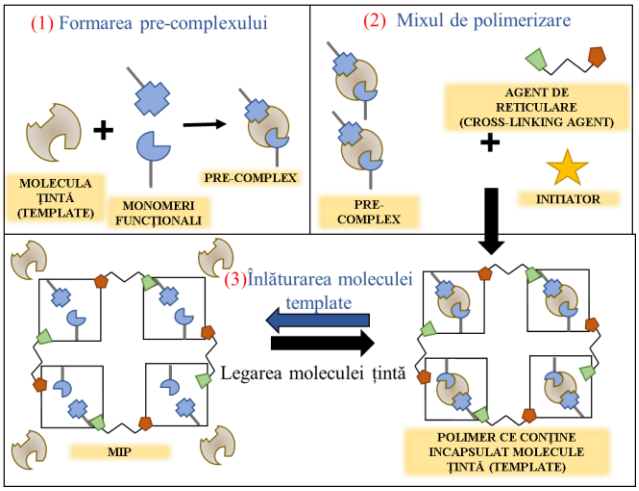

Figure 5.2. Schematic representation of the steps involved in the synthesis of MIPs.

Microcavities, capable of specific recognition of the target molecule, are formed in the structure of MIPs. The analytical signal enables sensitive and selective determinations using an appropriate detection device [33].

6. ELECTROCHEMICAL SENSORS BASED ON MIPs

Electrochemical sensors have gained remarkable importance in chemical analysis techniques due to their high sensitivity, low cost, rapid response and the possibility of being easily modified and miniaturized. Together with MIPs, they combine their advantages resulting in tools with high selectivity and sensitivity, increased chemical/mechanical stability with high reuse and low detection limits (LODs) [34], [35]. These characteristics are influenced by both the substrate type (only carbon-based electrodes are considered) and the modifiers, which act as the recognition element, being the detection nucleus of the sensor.

7. ELECTROCHEMICAL DETERMINATION OF OXYTETRACYCLINE USING PENCIL GRAPHITE ELECTRODE

The voltametric behavior of oxytetracycline at the pencil graphite electrode containing HB mine was investigated because it obtained the highest oxidation signal of OTC compared to other studied working electrodes (PGE of different hardness (2B, B, HB, H, 2H), GCE or Pt electrode).

During the development of the method, the influence of pH and nature of the support electrolyte on the voltametric process of OTC was studied, resulting in the oxidation of the antibiotic being characterized by an irreversible but pH-dependent electrode process. The results obtained by cyclic voltammetry differential pulsed voltammetry revealed that at OTC oxidation the number of electrons involved in the process is equal to the number of protons.

The linearity range of the DPV method developed for quantifying OTC in BRB pH = 4.56 at PGE, was between 1.0×10^{-6} to 3.6×10^{-4} mol/L OTC (figure 7.1.). The limit of detection (LOD) was 6.8×10^{-7} mol/L OTC and the limit of quantification (LOQ) $2.3 \times 10^{-6.}$ mol/L OTC.

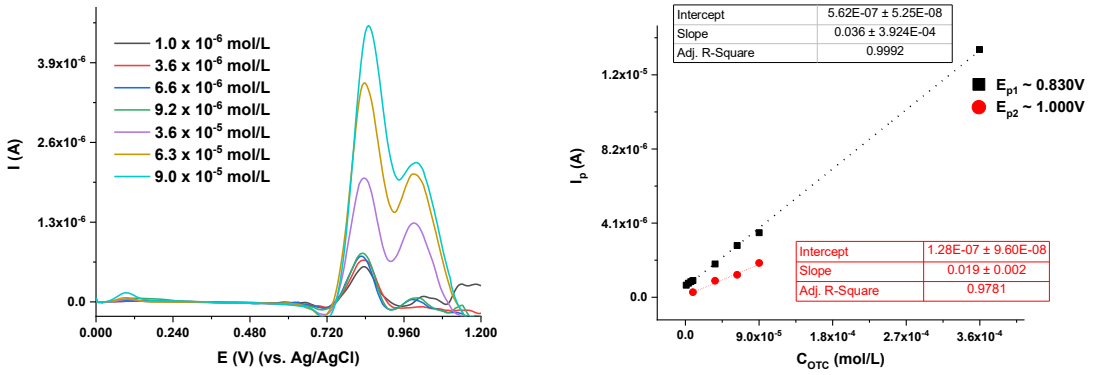

a) b)

Figure 7.1.a) Differential pulse voltammograms recorded at HB PGE for solutions of OTC of different concentrations in BRB pH solution = 4,56; b) variation in peak current intensity for different concentrations of OTC in BRB pH = 4,56.

The developed method is simple and fast, optimized for the determination of OTC in veterinary pharmaceuticals.

8. DETERMINATION OF DIPYRIDAMOLE USING MODIFIED PENCIL GRAPHITE ELECTRODES WITH MOLECULARLY PRINTED POLYMER FILMS

8.1.SELECTING THE MONOMER TO DEVELOP MOLECULARLY PRINTED POLYMER FILMS

- ***Naringin as a functional monomer***

It was studied the possibility of making a molecularly imprinted polymer film using dipyridamole as a template molecule. In this case naringin, a natural bioflavonoid whose chemical structure is shown in figure 8.1, was used as a functional monomer.

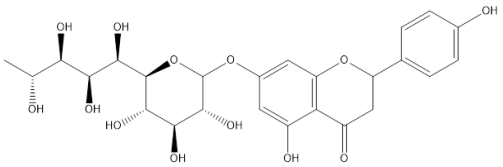

Figure 8.1. Structural formula of naringin.

Taking into account the literature data on the possibility of dimerization/polymerization of flavonoids at low pH with the possibility of loss of a proton and the production of a semiquinone radical [36], a potentiodynamic method was attempted to obtain a polynaringin film (pNGN). Following the optimization of the polymerization conditions for MIP and NIP and the use of newly formed sensors to measure the DIP-associated peak intensities in a solution containing 1,00 $\times 10^{-5}$ mol/L analyte, the sensor response was not satisfactory, so other monomers were considered.

- ***Gallic acid as a functional monomer***

Another functional monomer tested for the ability to form a molecular imprinted polymer film was gallic acid (GA), which is a tri-phenolic compound (figure 8.2) of biological and pharmacological importance having antibacterial, anticancer and anti-inflammatory properties.

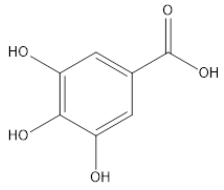

Figure 8.2. Structural formula of gallic acid

Starting from the fact that there are modified carbon electrodes with polygalic acid (pGA) in the literature, it was proposed to modify an electrode with gallic acid in 2 different electrolytic solutions: PBS pH = 7,00 and BRB pH = 9,00. The obtained sensors did not show superior qualities to the unmodified electrodes, so the working monomer was changed.

- ***Proflavin as a functional monomer***

Another monomer used to generate molecularly printed polymer films for DIP detection was proflavin (PFV), one of the most widely used antibacterial agents. Biological activity is given by its planar structure (figure 8.3), which can easily intercalate between the 2 helixes of DNA, thus blocking certain functions given by it [37].

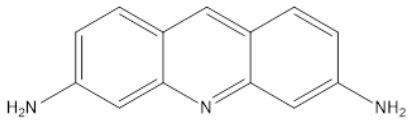

Figure 8.3. Structural formula of proflavin.

Two polymerization mixes were generated, the first containing PFV 2,00× 10^{-4} mol/L, for the purpose of forming the NIP and the other one containing the PFV 2,00 × 10^{-4} mol/L and DIP 2,00× 10^{-5} mol/L, for the formation of MIP. Were applied 5 potential cycles, in which it varied from - 0.300V to 1.300 V, and the scanning rate was 0.100V/. Even with the use of proflavin, the sensor response was not superior to the unmodified electrode.

8.2.DETERMINATION OF DIPYRIDAMOLE USING MODIFIED PGE WITH MIP BASED ON CAFFEIC ACID

In order to obtain the modified electrode MIP_PGE, a potentiodynamic polymerization method was used which consisted in applying 5 cycles of potential between 0,000 and 2,000V, the working solution containing CA (monomer), DIP (template) and PBS pH = 7,00 (supporting electrolyte). The same electrochemical treatment was applied to the supporting electrolyte, the electrode modified only with CA and the electrode modified with DIP. For the MIP_PGE electrode an appropriate CA (a) signal and a corresponding DIP (b) signal may be observed in the first voltammogram scan cycle, with anodic peaks being observed at approx. 0,300 V and ca. 0,500 V. During reverse scanning of the first potential cycle a cathode peak occurred at approx. 0,150 V. Since the 2nd cycle, these two signals have dropped dramatically, with the DIP signal (b)

disappearing completely since the 3rd cycle, while the corresponding CA signal (a) has shifted towards less positive potentials. According to Nian Bing Le et al. [38] this signal (from ca. 0.230 V) can be attributed to the formation of poly caffeic acid film (pCA). The redox couple of the anode signal with the cathode signal corresponding to the o-quinone/o-hydroquinone pair is evidence of pCA film formation [39], [40]. The improving peak currents with increasing the number of polymerization cycles suggested that the polymer generated at the electrode surface is conductive. DIP+CA polymerization voltammograms can be observed in Figure 8.4.

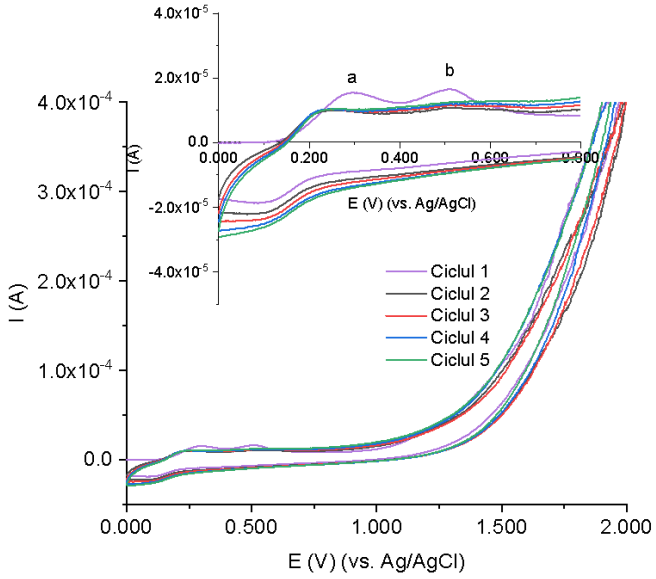

Figure 8.4. Cyclic voltammograms recorded at PGE during the electropolymerizing process having the reaction mix 2,00 × 10^{-4} mol/L and 4,00 × 10^{-5} mol/L DIP in PBS pH = 7,00, with a scan rate of 0,100 V/s. Inset: extended section of the region where CA and DIP signals were observed.

The experimental conditions for the development of the modified electrode were optimized by studying the influence of the concentration of the functional monomer and the template molecule, obtaining the optimal concentrations 2,00 × 10^{-4} mol/L CA and 4,00 × 10^{-5} mol/L DIP. It was determined that 5 voltametric cycles represent the optimal number of electropolymerizing cycles applied, the value of the scanning rate, namely 0.100 V/s, of the elimination conditions of the template molecule was determined and the electrode was characterized by electrochemical impedance spectroscopy.

The influence of the DIP concentration on the anode peak current obtained by DPV for MIP_PGE in PBS pH = 7,00 was studied in the concentration range 1,00 × 10^{-7} – 1,00 × 10^{-5} mol/L DIP and the peak currents in DPV were expressed according to the concentration of DIP in the solution, in PBS, pH = 7,00 (Figure 8.5).

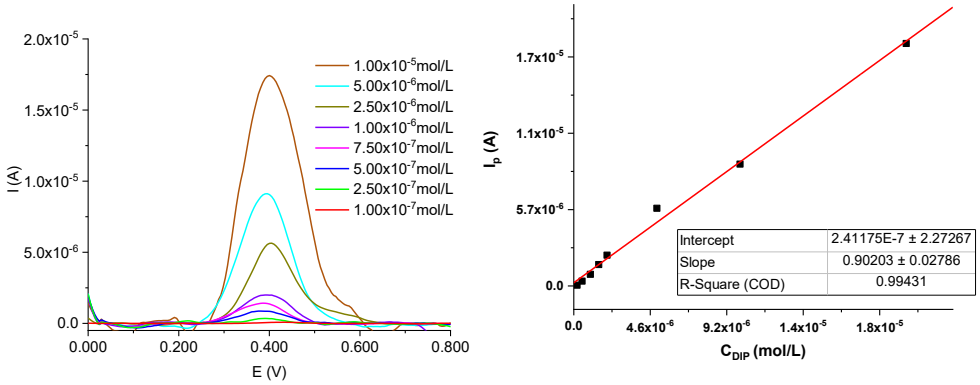

a) b)

Figure 8.5. a) DPV voltammogram at MIP_PGE for different concentrations of DIP in PBS pH = 7,00; b) representation of peak current intensities in DPV by solution DIP concentration in PBS, pH = 7,00 using scan rate of 0,100 V/s

Linear variation of the oxidation peak current with DIP concentration was described by the regression equation Ip (A) = 0,902× C_{DIP} (mol/L) + 2,412 × 10^{-7} (R^2 = 0,9943), which was valid for the entire concentration range investigated.

In order to reduce the lower limit of the linear range obtained for the DPV determination of the DIP at MIP_PGE, the influence of the accumulation of DIP at the electrode surface was studied by applying an accumulation time (t_{acc}) of 10 s and the scouring of the accumulation potential (E_{acc}) from −0,200 V to 0,200V. Taking into account that the highest oxidation peak current of the DIP was recorded at an E_{acc} of 0,200 V, in the next stage, this accumulation potential was maintained constant and t_{acc} was gradually increased up to 45 s. The oxidation signal DIP increased with increased t_{acc} up to 30 s and slightly decreased for longer periods of accumulation, most likely due to the saturation of the electrode surface with analyte molecules. DPV-Ads voltammograms were recorded for several analyte concentrations (figure 8.6).

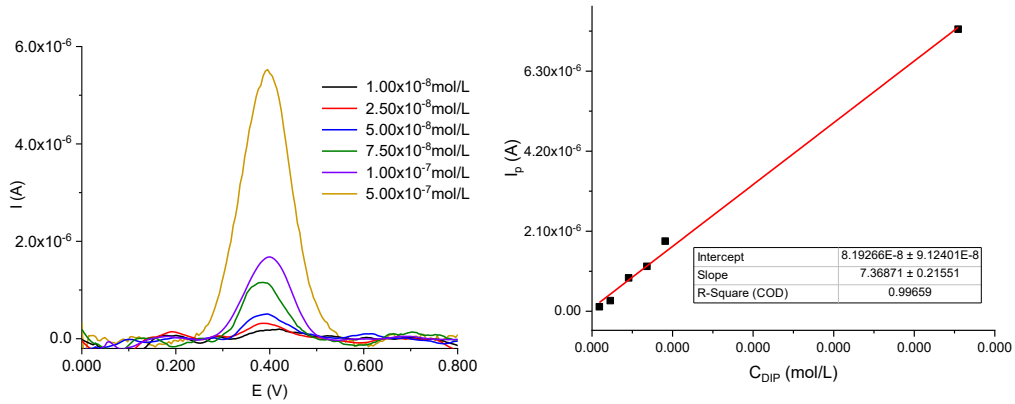

a) b)

Figure 8.6. a) Voltammograms obtained by Ads-DPV at MIP_PGE for different concentrations of DIP in PBS pH = 7,00, t_{acc} 30 s; E_{acc} 0,200 V; b) representation of peak currents intensities in the AdS-DPV technique according to the concentration of DIP in the solution, in PBS, pH 7,00 using the scanning rate of 0,100 V/s

Due to the electrocatalytic effect of pCA and the accumulation of analyte in selective MIP cavities, the irreversible pH-dependent anode signal of DIP was 28% higher at MIP_PGE compared to unchanged one.

The determination of DIP concentration was made by DPV, a more sensitive technique for modified PGE versus unchanged PGE, and not by AdS-DPV whose sensitivity was less than that of other sensors reported in the literature. However, linear ranges of almost two orders of magnitude and detection limits located at tens of nanomolar levels via DPV and AdS-DPV for MIP_PGE have demonstrated that they are suitable for quantifying DIP in pharmaceutical samples and human blood plasma when considering plasma DIP levels between 0,800 and 2,32 g/mL (1,58 $\times 10^{-6}$ to 4,60 $\times 10^{-6}$ mol/L) [41].

8.3. PENCIL GRAPHITE ELECTROCHEMICAL SENSOR BASED ON MOLECULARLY PRINTED FILM WITH CURCUMIN FOR DIPYRIDAMOLE DETECTION

The influence of the support electrolyte used in the electropolymerization phase on the amplitude of the DIP oxidation signal recorded at the PGE modified with the electropolymerized MIP in the appropriate environment, was investigated using HCl 0,1 mol/L, phosphate buffer

solution (PBS) pH = 7,00 and NaOH 0,2 mol/L, respectively (Table 8.1). In this respect, the potential applied to PGE was cycled five times between 0,000 and 1,000 V. The most intense signal was obtained when the surface of PGE was covered with PIP based on electropolymerized curcumin in NaOH 0,2 mol/L. Next, this environment was selected for further experiments.

Table 8.1. Anode peak currents, Ip (A), registered for DIP 1,00 × 10^{-5} mol/L in BRB pH = 3,29 by DPV with the electrode

The supporting electrolyte used to form the MIP film at PGE	**I_p (A)**
HCl 0,1 mol/L	5,76 × 10^{-6}
PBS pH = 7,00	6,98 × 10^{-6}
NaOH 0,2 mol/L	7,51 × 10^{-6}

For polymerization in NaOH 0,2 mol/L, at the anode scaling of the first potential cycle, the cyclical voltammogram recorded in strong basic environment for the CU and DIP mixture (Figure 8.7) showed an intense signal with peak potential of about 0,330 V, which also showed a weak pre-wave

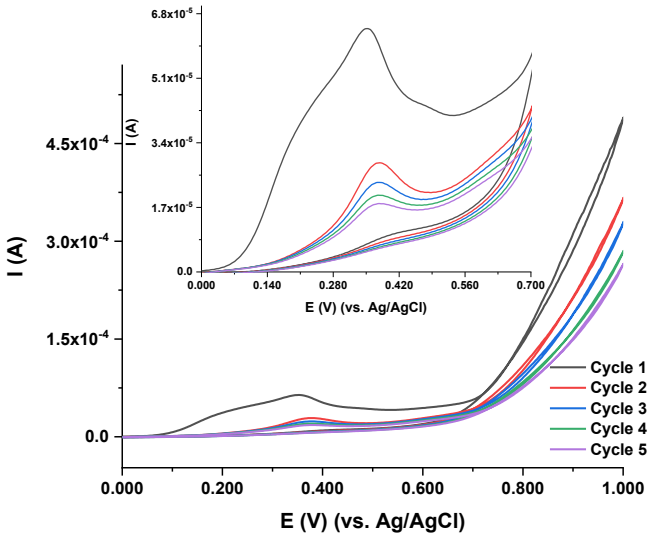

Figure 8.7. Cyclic voltammograms recorded at the PGE electrode for (a) 5,00 × 10^{-4} mol/L CU and (b) 5,00 × 10^{-4} mol/L CU in the presence of 2,50 × 10^{-5} mol/L DIP in NaOH 0,2 mol/L, scan rate 0,100 V/s. Inset: enlarged area of potential CU and DIP waves show signals.

During the development of the sensor, a number of relevant parameters were optimized, such as the ratio of monomer to template (2,00 × 10^{-5} mol/L and 4,00 × 10^{-5} mol/L, respectively), the number of potential cycles applied within the potentiodynamic electropolymerization (7 cycles), the speed of electropolymerization (0,100 V/s) and time of removal of the template molecule from the polymer film formed (120 minutes). Subsequently, molecularly imprinted polymer films were characterized by electrochemical impedance spectroscopy and from the point of view of the active surface.

The influence of DPV anode peak current was studied at MIP_PGE in BRB pH = 3.29 in concentration range 5,00 × 10^{-8} – 1,00 × 10^{-4} mol/L DIP (figure 8.8).

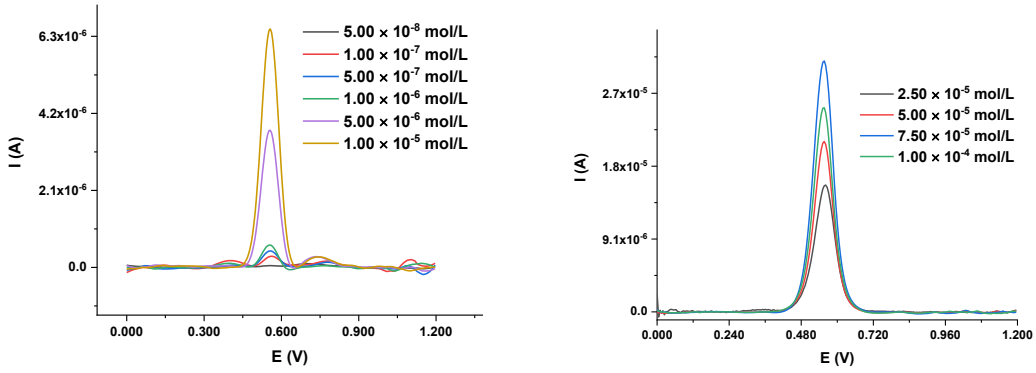

a) b)

Figure 10.2. a) Differential voltammograms with potential pulses recorded at MIP_PGE for DIP solutions of contractions ranging from 5,00 × 10^{-8} - 1,00 × 10^{-5} and b) 2,50 × 10^{-5} - 1,00 × 10^{-4} in BRB solution pH = 3,29 as a supporting electrolyte

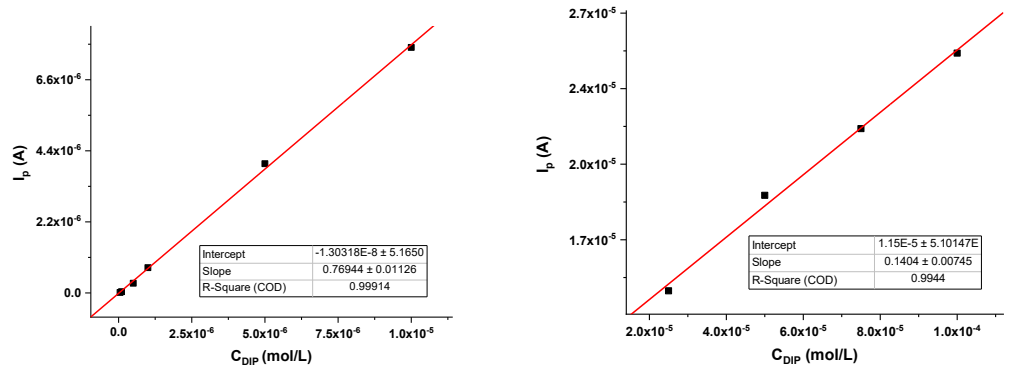

a) b)

Figure 10.3. a) Representation of peak currents in DPV by DIP concentration in solution for linear range $5{,}00 \times 10^{-8}$ – $1{,}00 \times 10^{-5}$ and b) $2{,}50 \times 10^{-5}$ – $1{,}00 \times 10^{-4}$ mol/L in BRB, pH = 3,29 using scan rate 0,100 V/s

Linear variation of peak oxidation current with DIP concentration is described by Ip regression equations (A) = $0{,}7341 \times C_{DIP}$ (mol/L) + $2{,}000 \times 10^{-8}$ ($R^2 = 0{,}9994$) for concentration range $5{,}00 \times 10^{-8}$ – $1{,}00 \times 10^{-5}$ and Ip (A) = $0{,}2016 \times C_{DIP}$ (mol/L) + $1{,}000 \times 10^{-5}$ ($R^2 = 0{,}9997$) for concentration range $2{,}50 \times 10^{-5}$ - $1{,}00 \times 10^{-4}$ mol/L.

A new electrochemical sensor based on MIP has been developed to identify the DIP, using CU as a monomer and DIP as a template molecule. Polymerization was based on a potentiodynamic method, obtaining an efficient and selective sensor for detecting DIP.

DPV and AdS-DPV electrochemical techniques were used to identify the DIP content in pharmaceutical tablets and tap water, resulting in a LOD of $1{,}47 \times 10^{-8}$ mol/L for DPV and $3{,}96 \times 10^{-9}$ mol/L for AdS-DPV and linear domains of almost two orders of magnitude $5{,}00 \times 10^{-8}$ - $1{,}00 \times 10^{-5}$ mol/L and $5{,}00 \times 10^{-9}$ - $1{,}00 \times 10^{-7}$ mol/L.

9. ENZYMATIC DEGRADATION OF DIPYRIDAMOLE IN THE PRESENCE OF LACASE AND USING CAFFEIC ACID AS MEDIATOR.

This chapter involved the use of polyphenols, previously used as functional monomers as enzyme mediators for the purpose of degradation of DIP. This study assessed the possible pollutant effect of the medicinal products in order to develop an enzymatic method of degradation of dipyridamole in the environment.

The first step was to study the influence of a fixed amount of lacase 0,20 mg/mL on the discoloration of a solution of DIP = $1{,}00 \times 10^{-4}$ mol/L, in ABS pH buffer solution = 4,40. Spectra resulting at varying time intervals can be observed in Figure 9.1.

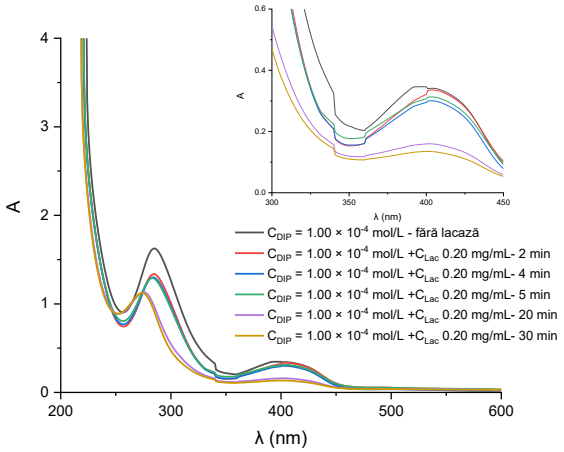

Figure 9.1. Dipyridamole degradation (DIP = 1,00 × 10^{-4} mol/L) in the presence of 0,20 mg/mL lacase recorded at different time periods.

From the spectra A = f(t), the maximum absorption in the VIS domain of DIP, namely 404 nm, could be determined, and subsequently from the interaction with the enzyme, its discoloration over time was observed. The optimal action pH of the enzyme was determined, overlaps with literature data (pH = 4,40).

Initial reaction rate V_R0 were determined as the slope of linear dependence per initial portion (approximately 200 seconds). The representation of the initial rate according to the initial concentration of DIP is shown in Figure 9.2.

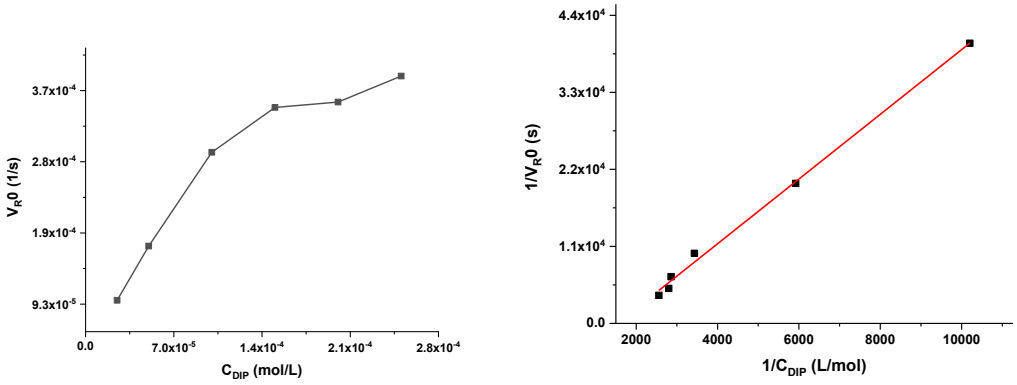

Figure 11.2. Representation of initial reaction speeds by DIP concentration and Linewaver-Burk linearization expressing relationship $1/V_R0 = f(1/C_{DIP})$

From the hyperbolic allure of the graph, it can be seen that the enzyme has a behavior typical of a Michaelis-Menten mechanism, the kinetic parameters being estimated from the Lineweaver-Burk graphical representation.

The influence of substrate concentration on enzymatic degradation was studied and the parameters Vmax = $1{,}41 \times 10^{-4}$ s^{-1} were estimated, and $K_M = 6{,}50 \times 10^{-5}$ mol/L. At the same time, the influence of the enzyme concentration in the context of enzymatic degradation was studied, observing a good linearity in the field studied. The influence of the CA mediator on the enzymatic reaction was also studied, observing its activation in small amounts of the mediator and a substrate competition for higher concentrations of caffeic acid.

10.CONCLUSIONS AND PERSONAL CONTRIBUTIONS

The electrochemical techniques based on unmodified carbon electrodes and modified with molecularly imprinted polymer films, based mainly on the detection of antibiotic and antithrombotic drugs from various sample matrices, were followed. To obtain rapid methods of analysis, the polymer film was obtained by an electrochemical method from a template (dipyridamole) and functional monomer (polyphenolic compounds). Two pencil graphite electrochemical carbon sensors with molecularly imprinted polymer films based on caffeic acid and curcumin have been developed. The parameters related to the synthesis of new polymer films were optimized and were characterized by electrochemical impedance spectroscopy and the electroactive surface was determined. Finally, the voltametric behavior of the sensors (influence of pH, scanning speed, analyte concentration, time and potential accumulation, etc.) was studied.

In chapter 7, the voltametric behavior of the OTC was studied. After establishing the working electrode, the influence of the supporting electrolyte and of the pH, it resulted that OTC is oxidized in an irreversible pH-dependent electrode process, was studied. The linearity range of the method is $1{,}0 \times 10^{-6} – 3{,}6 \times 10^{-4}$ mol/L OTC in BRB pH = 4,56. A limit of detection of $6{,}8 \times 10^{-7}$ mol/L OTC was obtained, which is suitable for determining OTC in veterinary pharmaceuticals.

Chapter 8 divides the results into **3 parts**. **In the first part**, suitable compounds were studied to be used as functional monomers in the polymerization process. Of these, naringin and gallic acid did not bring any improvement to the modified electrode, and proflavin brought an

improvement in the oxidation peak intensity of a solution of DIP 1.00 $\times 10^{-5}$ mol/L of Ip_{MIP} = 5,30 $\times 10^{-6}$ A, compared to Ip_{PGE} = 3,80 $\times 10^{-6}$ A. However, the best results are presented in the other parts of the chapter. **In the 2nd part,** DIP behavior was studied and using a modified disposable electrode with a molecular imprinted film deposited. The technique of obtaining the film was potentiodynamic electropolimerization of caffeic acid, together with the template molecule. Determination of the concentration of DIP was carried out by DPV, obtaining a linear range ranging from 1,00 $\times 10^{-7}$ – 1,00 $\times 10^{-5}$ mol/L with a limit of detection of 2,04 $\times 10^{-8}$ mol/L. Using an adsorptive striping technique, a linear domain was obtained that varies between 1,00 $\times 10^{-8}$ – 5,00 $\times 10^{-7}$ and has a limit of detection of 8,67 $\times 10^{-9}$ mol/L**. In the 3rd part,** a new electrochemical sensor based on curcumin-based MIP was presented to identify dipyridamole. Electropolymerization conditions have been optimized to obtain the best analytical signal. The extraction of the template molecule was carried out by immersing the electrode in EtOH for 2 hours. DPV and AdS-DPV techniques were used to identify the content of DIP, obtaining for each linear domain that spans almost 2 orders of magnitude 5,00 $\times 10^{-8}$ – 1,00 $\times 10^{-5}$ mol/L and 5,00 $\times 10^{-9}$ – 1,00 $\times 10^{-7}$ mol/L, showing the detection limits of 1,47 $\times 10^{-8}$ mol/LL for DPV and 3,96 $\times 10^{-9}$ mol/L for AdS-DPV respectively. The method was applied for the detection of dipyridamole in pharmaceutical preparations and tap water samples.

Chapter 9 presents the results of the ability to use polyphenol compounds as enzymatic mediators for the effective removal of dipyridamole from wastewater. The maximum absorption of DIP (404 nm) was determined from the initial spectra A = f(t) and subsequently the action of the enzyme on the substrate was tested over time. The optimal pH of the enzyme was determined (4,40), observing a good correlation with the one defined in the literature). The parameters V_{max} = 1,41 $\times 10^{-4}$ s^{-1} were determined, and K_M = 6,50 $\times 10^{-5}$ mol/L, as a result studied the influence of the substrate concentration on the enzymatic degradation. The possibility of enzyme inactivation was studied in a set concentration range (0,10 – 0,50 mg/mL), observing a good degree of linearity of the initial reaction rates depending on the enzyme concentration, resulting in the enzyme remaining active. The possibility of using CA as a mediator in the enzymatic degradation reaction was also studied, with an increase in the reaction speed to small amounts of the mediator and a substrate competition for higher concentrations of caffeic acid.

11.LIST OF PUBLICATIONS

ARTICLES PUBLISHED IN THE THESIS TOPIC

1. **D. Preda**, I. G. David, D. E. Popa, M. Buleandra, and G. L. Radu, "Recent Trends in the Development of Carbon-Based Electrodes Modified with Molecularly Imprinted Polymers for Antibiotic Electroanalysis," Chemosens. 2022, Vol. 10, Page 243, vol. 10, no. 7, p. 243, Jun. 2022, doi: 10.3390/CHEMOSENSORS10070243. (FI = 3.7)

2. **D. Preda**, M. L. Jinga, I. G. David, and G. L. Radu, "Determination of Dipyridamole Using a MIP-Modified Disposable Pencil Graphite Electrode," *Chemosensors*, vol. 11, no. 7, 2023, doi: 10.3390/chemosensors11070400.(FI = 3.7)

3. **D. Preda**, G. L. Radu, I. G. David, "Curcumin based MIP Electropolymerized on Single-Use Graphite Electrode for Dipyridamole Analysis" Molecules. 2024. Vol.29 , vol. 19, page 4630, https://doi.org/10.3390/molecules29194630 (FI= 4.6)

4. **D. Preda**, A.Matei, M-C. Cheregi, E-E. Iorgulescu, G. L. Radu, I. G. David Oxytetracycline electrochemical determination at disposable pencil graphite electrode, 2025, U.P.B. Sci. Bull., Seria B, Vol. 87, Iss. 1 (FI = 0.3)

Cumulative IF (1+2+3+4) = 12.3

INTERNATIONAL SCIENTIFIC COMMUNICATIONS ON THE TOPIC OF DOCTORAL THESIS

D. Preda, M. L. Jinga, G. L. Radu, I. G. David „Disposable MIP-based electrochemical sensor for sensitive determination of dypiridamole" - 10th conference „CHIMIA" 2024 Constanța, România, poster

D. Preda, A.Matei, M-C. Cheregi, E-E. Iorgulescu, G. L. Radu, I. G. David „Oxytetracycline analysis at disposable pencil graphite electrode" - 10th conference „CHIMIA" 2024 Constanța, România, poster

D. Preda, M. L. Jinga, G. L. Radu, G. I. David „Determination of dipyridamole by disposable MIP-based electrochemical sensor" – 23rd Romanian International Conference on Chemistry and Chemical Engineering, poster

M. L. Jinga, **D. Preda**, G. L. Radu, P. Oancea, A. Răducan „The influence of caffeic acid in laccase-dipyridamole system” - 10th conference „CHIMIA” 2024 Constanța, România, poster

12.BIBLIOGRAPHY

[1] M. Fáberová, I. Bodík, L. Ivanová, R. Grabic, and T. Mackuľak, “Frequency and use of pharmaceuticals in selected Slovakian town via wastewater analysis,” *Monatshefte fur Chemie*, vol. 148, no. 3, pp. 441–448, 2017, doi: 10.1007/s00706-016-1853-0.

[2] T. Grosser, S. Fries, and G. A. FitzGerald, “Biological basis for the cardiovascular consequences of COX-2 inhibition: Therapeutic challenges and opportunities,” *J. Clin. Invest.*, vol. 116, no. 1, pp. 4–15, 2006, doi: 10.1172/JCI27291.

[3] K. Ganesan, M. B. M. Rana, and S. Sultan, “Oral Hypoglycemic Medications,” *StatPearls*, May 2023, Accessed: Aug. 18, 2024. [Online]. Available: https://www.ncbi.nlm.nih.gov/books/NBK482386/.

[4] B. D. Abera *et al.*, “Laser-induced graphene electrodes modified with a molecularly imprinted polymer for detection of tetracycline in milk and meat,” *Sensors*, vol. 22, no. 1, pp. 1–17, 2022, doi: 10.3390/s22010269.

[5] F. Long, Z. Zhang, Z. Yang, J. Zeng, and Y. Jiang, “Imprinted electrochemical sensor based on magnetic multi-walled carbon nanotube for sensitive determination of kanamycin,” *J. Electroanal. Chem.*, vol. 755, pp. 7–14, 2015, doi: 10.1016/j.jelechem.2015.07.018.

[6] S. Haghdoust, U. Arshad, A. Mujahid, L. Schranzhofer, and P. A. Lieberzeit, “Development of a MIP-based QCM sensor for selective detection of penicillins in aqueous media,” *Chemosensors*, vol. 9, no. 12, 2021, doi: 10.3390/chemosensors9120362.

[7] R. López, S. Khan, A. Wong, M. del P. T. Sotomayor, and G. Picasso, “Development of a New Electrochemical Sensor Based on Mag-MIP Selective Toward Amoxicillin in Different Samples,” *Front. Chem.*, vol. 9, no. March, pp. 1–9, 2021, doi: 10.3389/fchem.2021.615602.

[8] C. R. Rawool and A. K. Srivastava, “A dual template imprinted polymer modified electrochemical sensor based on Cu metal organic framework/mesoporous carbon for highly sensitive and selective recognition of rifampicin and isoniazid,” *Sensors Actuators, B Chem.*, vol. 288, no. January, pp. 493–506, 2019, doi: 10.1016/j.snb.2019.03.032.

[9] S. Jafari, M. Dehghani, N. Nasirizadeh, and M. Azimzadeh, “An azithromycin electrochemical sensor based on an aniline MIP film electropolymerized on a gold nano urchins/graphene oxide modified glassy carbon electrode,” *J. Electroanal. Chem.*, vol. 829, no. June, pp. 27–34, 2018, doi: 10.1016/j.jelechem.2018.09.053.

[10] M. Dehghani, N. Nasirizadeh, and M. E. Yazdanshenas, “Determination of cefixime using a novel electrochemical sensor produced with gold nanowires/graphene oxide/electropolymerized molecular imprinted polymer,” *Mater. Sci. Eng. C*, vol. 96, no. June 2018, pp. 654–660, 2019, doi: 10.1016/j.msec.2018.12.002.

[11] C. Zhou, H. Zou, C. Sun, and Y. Li, “Recent advances in biosensors for antibiotic detection: Selectivity and signal amplification with nanomaterials,” *Food Chem.*, vol. 361, no. November 2020, p. 130109, 2021, doi: 10.1016/j.foodchem.2021.130109.

[12] Chara Calhoun1; Harrison R. Wermuth2; Gregory A. Hall3., *Antibiotics*. StatPearls Publishing, Treasure Island (FL), 2022.

[13] N. Drabińska *et al.*, “Application of a solid-phase microextraction-gas chromatography-mass spectrometry/metal oxide

sensor system for detection of antibiotic susceptibility in urinary tract infection-causing Escherichia coli – A proof of principle study," *Adv. Med. Sci.*, vol. 67, no. 1, pp. 1–9, 2022, doi: 10.1016/j.advms.2021.09.001.

[14] A. G. Ayankojo, J. Reut, V. Ciocan, A. Öpik, and V. Syritski, "Molecularly imprinted polymer-based sensor for electrochemical detection of erythromycin," *Talanta*, vol. 209, no. July 2019, p. 120502, 2020, doi: 10.1016/j.talanta.2019.120502.

[15] C. Foti, A. Piperno, and A. Scala, "Oxazolidinone Antibiotics: Chemical, Biological and Analytical Aspects," *Molecules*, vol. 26, no. 14, pp. 4280–4293, 2021, doi: https://doi.org/10.3390/molecules26144280.

[16] M. Torkashvand, M. B. Gholivand, and G. Malekzadeh, "Construction of a new electrochemical sensor based on molecular imprinting recognition sites on multiwall carbon nanotube surface for analysis of ceftazidime in real samples," *Sensors Actuators, B Chem.*, vol. 231, pp. 759–767, 2016, doi: 10.1016/j.snb.2016.03.061.

[17] F. Schneider, A. Gessner, and N. El-Najjar, "Efficacy of Vancomycin and Meropenem in Central Nervous System Infections in Children and Adults: Current Update," *Antibiotics*, vol. 11, no. 2, pp. 173–195, 2022, doi: 10.3390/antibiotics11020173.

[18] W. da Silva, A. C. Queiroz, and C. M. A. Brett, "Poly(methylene green) – Ethaline deep eutectic solvent / Fe2O3 nanoparticle modified electrode electrochemical sensor for the antibiotic dapsone," *Sensors Actuators, B Chem.*, vol. 325, no. June, p. 128747, 2020, doi: 10.1016/j.snb.2020.128747.

[19] R. Ding *et al.*, "Recent advances in quantum dots-based biosensors for antibiotic detection," *J. Pharm. Anal.*, no. xxxx, 2021, doi: 10.1016/j.jpha.2021.08.002.

[20] S. G. Surya *et al.*, "A chitosan gold nanoparticles molecularly imprinted polymer based ciprofloxacin sensor," *RSC Adv.*, vol. 10, no. 22, pp. 12823–12832, 2020, doi: 10.1039/d0ra01838d.

[21] I. A. Stoian *et al.*, "Biomimetic electrochemical sensor for the highly selective detection of azithromycin in biological samples," *Biosens. Bioelectron.*, vol. 155, no. November 2019, p. 112098, 2020, doi: 10.1016/j.bios.2020.112098.

[22] P. Rebelo, J. G. Pacheco, I. V Voroshylova, A. Melo, M. N. D. S. Cordeiro, and C. Delerue-Matos, "Rational development of molecular imprinted carbon paste electrode for Furazolidone detection: theoretical and experimental approach," *Sensors Actuators, B Chem.*, vol. 329, no. July 2020, 2021, doi: 10.1016/j.snb.2020.129112.

[23] K. K. Wu and N. Matijevic-Aleksic, "Molecular aspects of thrombosis and antithrombotic drugs," *Crit. Rev. Clin. Lab. Sci.*, vol. 42, no. 3, pp. 249–277, 2005, doi: 10.1080/10408360590951171.

[24] M. Thangaraj and R. Kuber, "UPLC-Q-TOF-MS method development and validation for simultaneous analysis of dipyridamole and its related impurities," *J. Appl. Pharm. Sci.*, vol. 13, no. 1, pp. 201–211, Jan. 2023, doi: 10.7324/JAPS.2023.130120.

[25] "Electrochemical Sensors Based on Carbon Composite Materials," *Electrochem. Sensors Based Carbon Compos. Mater.*, Sep. 2022, doi: 10.1088/978-0-7503-5127-0.

[26] E. Vacalie, D. Preda, P. Oancea, A. R. Leonties, L. Aricov, and A. Raducan, "Effective degradation of azo dyes by ABTS (2,2'-azino-bis (3-ethylbenzothiazoline-6-sulfonic acid)) mediated laccase. Kinetic studies," *Process Biochem.*, vol. 145, pp. 311–319, Oct. 2024, doi: 10.1016/J.PROCBIO.2024.07.011.

[27] Ž. Z. Tasić, M. B. Petrović Mihajlović, A. T. Simonović, M. B. Radovanović, and M. M. Antonijević, "Review of applied surface modifications of pencil graphite electrodes for paracetamol sensing," *Results Phys.*, vol. 22, p. 103911, Mar. 2021, doi: 10.1016/J.RINP.2021.103911.

[28] X. Liu *et al.*, "Recent advances in sensors for tetracycline antibiotics and their applications," *TrAC Trends Anal. Chem.*, vol. 109, pp. 260–274, Dec. 2018, doi: 10.1016/J.TRAC.2018.10.011.

[29] Z. Long Ma, M. Chen Wang, L. Tian, and L. Cheng, "A multi-responsive luminescent indicator based on a Zn(II) metal-organic framework with 'Turn on' sensing of pyridine and 'Turn off' sensing of Fe3+, Cr2O72− and antibiotics in aqueous media," *Inorganica Chim. Acta*, vol. 526, no. July, p. 120513, 2021, doi: 10.1016/j.ica.2021.120513.

[30] L. Wang and Y. Tang, "Determination of dipyridamole using TCPO-H2O2 chemiluminescence in the presence of silver nanoparticles," *Luminescence*, vol. 26, no. 6, pp. 703–709, 2011, doi: 10.1002/bio.1301.

[31] R. I. Boysen, L. J. Schwarz, D. V Nicolau, and M. T. W. Hearn, "Molecularly imprinted polymer membranes and thin films for the separation and sensing of biomacromolecules," *J. Sep. Sci.*, vol. 40, no. 1, pp. 314–335, Jan. 2017, doi: https://doi.org/10.1002/jssc.201600849.

[32] Y. Zhang, Z. Liu, Y. Wang, X. Kuang, H. Ma, and Q. Wei, "Directly assembled electrochemical sensor by combining self-supported CoN nanoarray platform grown on carbon cloth with molecularly imprinted polymers for the detection of Tylosin," *J. Hazard. Mater.*, vol. 398, no. April, p. 122778, 2020, doi: 10.1016/j.jhazmat.2020.122778.

[33] L. Xie, N. Xiao, L. Li, X. Xie, and Y. Li, "Theoretical insight into the interaction between chloramphenicol and functional monomer (Methacrylic acid) in molecularly imprinted polymers," *Int. J. Mol. Sci.*, vol. 21, no. 11, pp. 1–14, 2020, doi: 10.3390/ijms21114139.

[34] A. N. Hasanah, N. Safitri, A. Zulfa, N. Neli, and D. Rahayu, "Factors affecting preparation of molecularly imprinted polymer and methods on finding template-monomer interaction as the key of selective properties of the materials," *Molecules*, vol. 26, no. 18, pp. 5612–5634, 2021, doi: 10.3390/molecules26185612.

[35] N. Leibl, K. Haupt, C. Gonzato, and L. Duma, "Molecularly imprinted polymers for chemical sensing: A tutorial review," *Chemosensors*, vol. 9, no. 6, pp. 1–19, 2021, doi: 10.3390/chemosensors9060123.

[36] G. Ziyatdinova, E. Yakupova, E. Ziganshina, and H. Budnikov, "First Order Derivative Voltammetry on the in situ Surfactant Modified Electrode for Naringin Quantification," *Electroanalysis*, vol. 31, no. 11, pp. 2130–2137, 2019, doi: 10.1002/elan.201900257.

[37] A. Porfireva and G. Evtugyn, "Electrochemical DNA sensor based on the copolymer of proflavine and Azure B for doxorubicin determination," *Nanomaterials*, vol. 10, no. 5, p. 924, May 2020, doi: 10.3390/nano10050924.

[38] B. L. Nian, W. Ren, and Q. L. Hong, "Caffeic Acid-Modified Glassy Carbon Electrode for the Simultaneous Determination of Epinephrine and Dopamine," *Electroanalysis*, vol. 19, no. 14, pp. 1496–1502, Jul. 2007, doi: 10.1002/ELAN.200703871.

[39] P. T. Lee, K. R. Ward, K. Tschulik, G. Chapman, and R. G. Compton, "Electrochemical Detection of Glutathione Using a Poly(caffeic acid) Nanocarbon Composite Modified Electrode," *Electroanalysis*, vol. 26, no. 2, pp. 366–373, Feb. 2014, doi: 10.1002/ELAN.201300486.

[40] A. Rohanifar, A. M. Devasurendra, J. A. Young, and J. R. Kirchhoff, "Determination of L-DOPA at an optimized poly(caffeic acid) modified glassy carbon electrode," *Anal. Methods*, vol. 8, no. 44, pp. 7891–7897, Nov. 2016, doi: 10.1039/C6AY01873D.

[41] A. Dresse *et al.*, "Pharmacokinetics of oral dipyridamole (Persantine®) and its effect on platelet adenosine uptake in man," *Eur. J. Clin. Pharmacol.*, vol. 23, no. 3, pp. 229–234, May 1982, doi: 10.1007/BF00547559/METRICS.